Analysis of ridge formation

Kjær-Pedersen, N.

Publication date:
1973

Document Version
Publisher's PDF, also known as Version of record

A. E. K. Risø

Risø - M - 1625

Risø - M - 1625

Title and author(s)

Analysis of Ridge Formation

by

Niels Kjær-Pedersen

Date June 15, 1973

Department or group

Metallurgy Dept.

Group's own registration number(s)

A-175

16 pages + tables + illustrations

Abstract

A mathematical model is discussed, which analyses the elastic and plastic deformation of a tube under a specified local load applied axisymmetrically to the inner tube surface. The model accounts for anisotropic plastic properties of the materials. Creep behaviour during irradiation is described by Nichols' model. Numerical results have been obtained by means of a digital computer. A discussion of these results is given.

Copies to

A.R. Mackintosh
C.F. Jacobsen
M. Møller-Madsen
Metallurgy Dept.(40)
Library (100)

ISBN-87 550 0204 8

Risø-M-1625

ANALYSIS OF RIDGE FORMATION

by

Niels Kjær-Pedersen
Elsinore Shipyard and Engineering Co.
Elsinore, Denmark

Work performed under contract with the Danish Atomic Energy Commission,
Risø, 4000 Roskilde, Denmark.

Contents

1. Definition of the Problem

During irradiation in a reactor a fuel pellet expands and exerts a pressure on the cladding tube. Since the pellet tends to assume an hour-glass shape the ends of adjacent pellets in the tube will tend to deform the tube so as to create a circumferential ridge.

In many cases the pellet will crack longitudinally in which case the force distribution will not be axisymmetric. However, in this approach we shall assume that no such cracks form, i.e. the force distribution is assumed to be axisymmetric.

As the pellets change their volume and shape they may not only exert a normal force on the tube surface but also a friction force which, due to the assumption of axisymmetry will be oriented in the axial direction.

We shall assume that any two adjacent pellets behave likewise, i.e. the ridge as well as the force distribution will be symmetric with respect to the pellet end cross-section.

Fig. 1. illustrates how the situation is conceived. The tube is shown in a longitudinal section, in the deformed situation. Only the lower half of the ridge is shown. A length L is introduced, rather arbitrarily, to specify some axial distance from the ridge top beyond which the force distribution is zero, except for the uniform inner and outer gas pressures.

Included in fig. 1 is a plot of the assumed force distributions which act on the inner tube surface. K_n denotes the normal force per unit area, K_s the friction force per unit area. K_n and K_s are symmetric with respect to the s-axis. K_s is zero at $t = 0$, while both K_n and K_s are zero at $t = 1$.

Besides the mechanical forces there will be an effect of the temperature distribution throughout the material considered.

Rigorous treatment of the problem as stated requires the solution of the thermo-visco-elastic equations in cylindrical coordinates for the axisymmetric case. This again requires information about elastic constants, thermal expansion coefficient, plastic deformation anisotropy constants and an empirical model for the creep of the material under

the influence of fast flux, fluence, effective stress and strain, temperature, etc.

2. Definition of the Mathematical Model

Due to the complexity of the system equations, a rigorous solution is not obtainable.

In order to determine an approximate solution, the deformations u and w are expressed as fourth-order polynomial forms in the two coordinates s and t, which are defined in fig. 1.

The order of the polynomial forms has been chosen such as to provide a suitable number of coefficients to be determined by application of what is considered a reasonable set of boundary conditions.

Clearly, the second-order differential equations which describe the state of deformation in cylindrical coordinates are not satisfied by any polynomial forms. Hence, the success of the method rests entirely on the choice of appropriate boundary conditions.

Since the creep model is of empirical nature and as such not readily compatible with the polynomial approximation technique, it is necessary to use a fitting procedure to link the creep model to the over-all model.

3. Description of the Model

3.1. Thermo-Elastic Equations in Cylindrical Coordinates

The general elastic equations of motion in cylindrical coordinates read:

$$(1)\quad \frac{\sigma_r-\sigma_\theta}{r} + \frac{\partial \sigma_r}{\partial r} + \frac{\partial \sigma_{ar}}{\partial z} + \frac{1}{r}\frac{\partial \sigma_{\theta r}}{\partial \theta} + \beta_r = \rho \ddot{u}$$

$$(2)\quad \frac{1}{r}\left(\frac{\partial \sigma_\theta}{\partial \theta} + 2\,\sigma_{r\theta}\right) + \frac{\partial \sigma_{a\theta}}{\partial z} + \frac{\partial \sigma_{r\theta}}{\partial r} + \beta_\theta = \rho \ddot{v}$$

$$(3)\quad \frac{1}{r}\left(\frac{\partial \sigma_{\theta a}}{\partial \theta} + \sigma_{ra}\right) + \frac{\partial \sigma_a}{\partial z} + \frac{\partial \sigma_{ra}}{\partial r} + \beta_a = \rho \ddot{w}$$

The stresses are expressed by the elastic strains and the temperature variation:

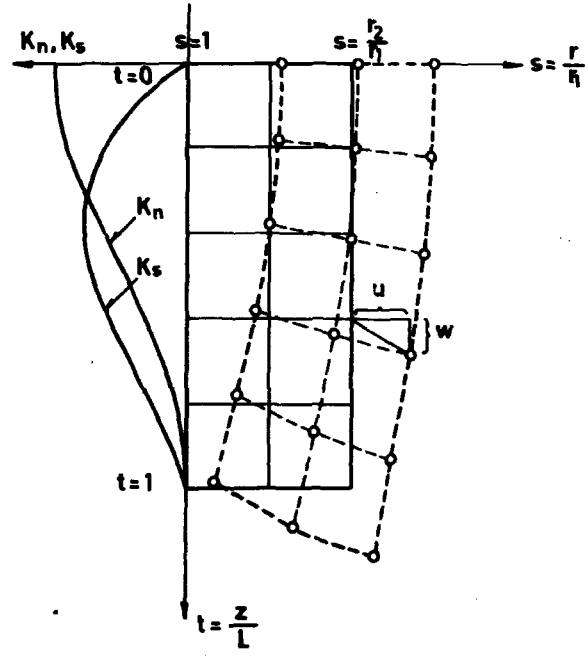

Figure 1.

Tube wall in deformed situation

$$(4)\quad \sigma_a = A\left\{1_a(1-\nu) + \nu(1_\theta + 1_r) - (1+\nu)\,\alpha\,T\right\}$$

$$(5)\quad \sigma_\theta = A\left\{1_\theta(1-\nu) + \nu(1_r + 1_a) - (1+\nu)\,\alpha\,T\right\}$$

$$(6)\quad \sigma_r = A\left\{1_r(1-\nu) + \nu(1_a + 1_\theta) - (1+\nu)\,\alpha\,T\right\}$$

$$(7)\quad \sigma_{a\theta} = B\,1_{a\theta}$$

$$(8)\quad \sigma_{\theta r} = B\,1_{\theta r}$$

$$(9)\quad \sigma_{ra} = B\,1_{ra}$$

The total strains are expressed by the local deformations:

$$(10)\quad \varepsilon_r = \frac{\partial u}{\partial r}$$

$$(11)\quad \varepsilon_\theta = \frac{u}{r} + \frac{1}{r}\frac{\partial v}{\partial \theta}$$

$$(12)\quad \varepsilon_a = \frac{\partial w}{\partial z}$$

$$(13)\quad \varepsilon_{a\theta} = \frac{1}{2}\left(\frac{\partial v}{\partial z} + \frac{1}{r}\frac{\partial w}{\partial \theta}\right)$$

$$(14)\quad \varepsilon_{\theta r} = \frac{1}{2}\left(\frac{\partial v}{\partial r} + \frac{1}{r}\frac{\partial u}{\partial \theta} - \frac{v}{r}\right)$$

$$(15)\quad \varepsilon_{ra} = \frac{1}{2}\left(\frac{\partial w}{\partial r} + \frac{\partial u}{\partial z}\right)$$

The relationship between total and elastic strain is:

$$(16)\quad \varepsilon_{ij} = 1_{ij} + e_{ij}$$

If the plastic strains are known at any particular time, it is in principle possible to solve for the elastic state of deformation by substituting eqs. (16) into eqs. (10) through (15), eqs. (10) through (15) into eqs. (4) through (9), eqs. (4) through (9) into eqs. (1) through (3). This gives 3 second-order differential equations in u, v, w.

3.2. Anisotropic Theory of Plasticity

Hill[1] has formulated a theory of plastic deformation of anisotropic materials based on von Mises[2] idea of a plastic potential.

The equations are:

$$(17)\quad \dot{e}_a = P\left\{F(\sigma_a-\sigma_\theta) - H(\sigma_r-\sigma_a)\right\}$$

$$(18)\quad \dot{e}_\theta = P\left\{G(\sigma_\theta-\sigma_r) - F(\sigma_a-\sigma_\theta)\right\}$$

$$(19)\quad \dot{e}_r = P\left\{H(\sigma_r-\sigma_a) - G(\sigma_\theta-\sigma_r)\right\}$$

$$(20)\quad \dot{e}_{a\theta} = P\left\{L\,\sigma_{a\theta}\right\}$$

$$(21)\quad \dot{e}_{\theta r} = P\left\{M\,\sigma_{\theta r}\right\}$$

$$(22)\quad \dot{e}_{ra} = P\left\{N\,\sigma_{ra}\right\}$$

$$(23)\quad P = \dot{e}_g(\sigma_g)/\sigma_g$$

$$(24)\quad \sigma_g = \left\{F(\sigma_a-\sigma_\theta)^2 + G(\sigma_\theta-\sigma_r)^2 + H(\sigma_r-\sigma_a)^2 + 2L\sigma_{a\theta}^2 + 2M\sigma_{\theta r}^2 + 2N\sigma_{ra}^2\right\}^{\frac{1}{2}}$$

σ_g is named the effective stress.

It is noted that $\dot{e}_a + \dot{e}_\theta + \dot{e}_r = 0$, reflecting the idea that there can be no plastic dilatation.

F, G, H, L, M, N are named the constants of anisotropy.

The quantity P corresponds to the elastic modulus of the theory of elasticity. It is primarily a function of σ_g but depends also on various other parameters, like temperature, mechanical and heat treatment, irradiation level, irradiation history, etc.

3.3. Creep Model by Nichols

There does not exist a generally accepted theory for the irradiation-enhanced creep of metals. Nichols[3], however, has compiled a model which is widely used and probably gives reasonable results.

Basically, the model gives the quantity P of the previous section as a function of effective stress, temperature, neutron flux and integrated flux as well as a number of materials parameters.

Nichols' model is based on empirical relationships and can be adapted to represent almost any currently accepted truth.

3.4. The Equations in the Axisymmetric Case

Eqs. (4) through (9) become in axial symmetry:

$$(25)\quad \sigma_a = A\left\{1_a(1-\nu) + \nu(1_\theta+1_r) - (1+\nu)\,\alpha\,T\right\}$$

$$(26)\quad \sigma_\theta = A\left\{1_\theta(1-\nu) + \nu(1_r+1_a) - (1+\nu)\,\alpha\,T\right\}$$

(27) $\sigma_r = A\{1_r(1-\nu) + \nu(1_a+1_\theta) - (1+\nu)\ \alpha T\}$

(28) $\sigma_{ra} = B\ 1_{ra}$

Eqs. (10) through (15) become:

(29) $\varepsilon_r = \frac{\partial u}{\partial r}$

(30) $\varepsilon_\theta = \frac{u}{r}$

(31) $\varepsilon_a = \frac{\partial w}{\partial z}$

(32) $\varepsilon_{ra} = \frac{1}{2}(\frac{\partial w}{\partial r} + \frac{\partial u}{\partial z})$

3.5. The Polynomial Approach

The local deformations u and w are expressed by the following polynomial forms:

(33) $u = a_{40}s^4 + a_{31}s^3t + a_{22}s^2t^2 + a_{13}st^3 + a_{04}t^4 + a_{30}s^3 + a_{21}s^2t + a_{12}st^2 + a_{03}t^3 + a_{20}s^2 + a_{11}st + a_{02}t^2 + a_{10}s + a_{01}t + a_{00}$

(34) $w = b_{40}s^4 + \text{etc.}$

Similarly for the plastic deformations, we define:

(35) $up = ap_{40}s^4 + \text{etc.}$

(36) $wp = bp_{40}s^4 + \text{etc.}$

The idea behind the present approach is to apply the set of boundary conditions discussed in the next paragraph to the above polynomial forms, making proper use of eqs. (16) through (32).

This permits us for any known set of ap_{ij} and bp_{ij} to establish a set of 30 eqs. for the determination of the corresponding a_{ij} and b_{ij}.

Once the a_{ij} and b_{ij} are known the stress state is also known and hence the rate of plastic deformation may be determined in any point. This is carried out by applying Nichols' model to a number of points throughout the material.

When the $\dot{e}_\theta$, $\dot{e}_r$ and $\dot{e}_{ar}$ have been determined, the values are used for the fitting of the polynomial coefficient change rates $\dot{ap}_{ij}$ and $\dot{bp}_{ij}$ by means of an rms criterion.

Finally, when the $\dot{ap}_{ij}$ and $\dot{bp}_{ij}$ are known an integration can be performed over a time interval to give a new state of plastic deformation.

At this point a new state of elastic deformation and a new evaluation of the plastic deformation rate can be worked out so that another time-step may be taken, etc. etc.

3.6. Discussion of Boundary Conditions

Fifteen boundary conditions have been used in the model. In the following, each of them will be briefly explained.

Condition I

Axial symmetry at t = 0:

$$\frac{\partial u(s,0)}{\partial t} = \frac{\partial up(s,0)}{\partial t} = 0$$

$$w(s,0) = wp(s,0) = 0$$

This condition causes 9 of the a_{ij} and b_{ij} and 9 of the ap_{ij} and bp_{ij} to vanish.

Condition II

Zero plastic dilatation at any point:

$$\frac{\partial up(s,t)}{\partial r} + \frac{up(s,t)}{r} + \frac{\partial wp(s,t)}{\partial z} = 0$$

This condition causes 7 of the ap_{ij} and bp_{ij} to vanish and yields another 7 equations among the ap_{ij} and bp_{ij}.

Condition III

The normal stress at the outer surface matches the external pressure:

$$\sigma_r(x,t) = -p_2$$

This condition yields 5 equations among the a_{ij} and b_{ij}.

Condition IV

The shear stress vanishes at the outer surface:

$$\sigma_{ar}(s,t) = 0$$

This condition yields 3 equations.

Condition V

The normal stress at the inner surface matches the normal force from the fuel plus the internal pressure:

$$\sigma_r\ (1,t) = -\ (p_1 + K_n)$$

This condition yields 4 equations.

Condition VI

The shear stress at the inner surface matches the friction force from the fuel:

$$\sigma_{ar}\ (1,t) = -\ K_s$$

This condition yields 2 equations

Condition VII

The axial tension, averaged over the ridge top cross-section, equals a specified value:

$$\int_{r_1}^{r_2} \sigma_a\ (s,0)\ dr = \frac{1}{2}\ (r_2^{\,2} - r_1^{\,2})\ \sigma_{ao}$$

This condition yields one equation.

Condition VIII

The axial tension, averaged over the cross-section, decreases as t goes from 0 to 1 by an amount equal to the total fuel friction force:

$$\int_{r_1}^{r_2} \sigma_a\ (s,0)\ rdr - \int_{r_1}^{r_2} \sigma_a\ (s,1)\ rdr = r_1 \int_0^L K_s\ dz$$

This condition yields one equation.

Condition IX

Total radial force balance:

$$\int_0^L \int_{r_1}^{r_2} \sigma_0(s,t)\ drdz = r_1 \int_0^L (p_1 + K_n - p_2)dz + \int_{r_1}^{r_2} \sigma_{ar}(s,1)\ rdr$$

This condition yields one equation.

Condition X

The interface at t = 1 is assumed to connect with an infinite tube subjected to the same inner and outer pressures and to a temperature increase equal to the average of that of the interface.

This tube deforms in the radial direction approximately according to an exponential law, apart from the base deformation due to pressure and temperature. The shear stress corresponding to the elastic part of this deformation must match the average shear stress at t = 1. Further, the surfaces must be smooth at the junction.

This condition yields 3 equations.

Condition XI

Moment balance.

Let M_1 denote the moment of the axial stresses at the t = 0 cross-section, positive counter-clockwise, and M_2 the corresponding moment at the t = 1 cross-section, positive clockwise. Further, let M_h denote the moment of the hoop stress with respect to the t = 1 cross-section, positive clockwise, and M_x the moment of the external force with respect to the inner surface cross-sectional tangent line at t = 1, positive clockwise.

We then have:

$$M_1 - M_2 = M_h + M_x$$

This condition yields one equation.

Condition XII

Energy minimization.

The internal elastic energy is given by

$$W = \frac{4\pi G}{1-2\nu} \int_0^L \int_{r_1}^{r_2} \left\{ \frac{1-2\nu}{2}\ (1_a^{\,2} + 1_r^{\,2} + 1_\theta^{\,2} + 2 1_{ar}^{\,2}) + \frac{\nu}{2}\ (1_a + 1_r + 1_\theta)^2 - (1+\nu)\ \alpha T\ (1_a + 1_r + 1_\theta) \right\} rdrdz$$

Minimization of this expression with respect to a selected coefficient yields one quation.

In this model minimization is performed with respect to a_{10} and b_{01}, i.e. two equations are obtained.

Condition XIII

Shear stress minimization.

The average square of the shear stress is proportional to

$$T = \int_0^L \int_{r_1}^{r_2} \left\{ \left(\frac{\partial w}{\partial r} + \frac{\partial u}{\partial z}\right) - \left(\frac{\partial vp}{\partial r} + \frac{\partial up}{\partial z}\right) \right\}^2 rdrdz$$

Minimization of this quantity with respect to b_{21} and b_{11} yields two equations.

Condition XIV

Specified moment of axial stress at z = L.

If the axial stress were evenly distributed across the cross-section it would have moment zero with respect to some radial distance r_o. We now impose on the actual stress distribution that it have a specified moment M_2 with respect to r_o.

Condition XV

Specified axial stress distribution at z = L.

This condition yields 5 equations.

4. Short Description of the Code

4.1. General

The equations, derived from the 15 boundary conditions and the application of the creep model, have been coded into a computer programme named RIDGE.

This programme starts from a situation of no deformation, then applies a prescribed set of forces and a prescribed temperature distribution in order to obtain a state of stress, a state of elastic deformation and a distribution of plastic deformation rates.

It then goes on to integrate the plastic deformation rates over a prescribed time step, taking into account a set of forces and a temperature distribution prescribed for the new point in time. An iteration is performed so that the plastic deformation rates used in the integration process equal the averages of those calculated at the end points of the time step.

4.2. Options

The 15 boundary conditions discussed in paragraph 3.6 provide an overcomplete set of equations for the determination of the coefficients.

For a particular case, judgement must be exercised to select a suitable subset of boundary conditions.

For the present, the following options are available in the model:

IPEL / IOPT	0	1	2
0	Cond's. XII through XV deleted. Cond. X partly deleted. x) $a_{oo} = a_{40} = 0$	Cond's XII through XV deleted. Cond. X modified to secure zero average shear at z = L. $a_{oo} = a_{40} = 0$	
1	Cond's. X and XIII through XV deleted $a_{oo} = 0$		Cond's. X, XII, XIV and XV deleted. $a_{oo} = 0$
2	Conditions XII through XV deleted	Cond's. VII through XI, XIII and XIV deleted	Cond's. X, XIII and XV deleted.

x) Cond. X in this case neglects the condition that the surfaces must be smooth at the junction.

The options are selected by means of the two input integers, IOPT and IPEL.

As it appears from the table, in some cases one or two coefficients are arbitrarily put to zero in order to maintain the balance of the equations.

To calculate a ridge, one should select IOPT = 2, IPEL = 0.

To calculate a free pellet, one should select IOPT = 2, IPEL = 1. The remaining options have been valuable during the checking of the model. They have been retained because some of them are practical in special cases.

4.3. Time step Selection

The convergence properties of the code seem rather promising. A time step of 100 hours has been successfully performed with a fuel normal force big enough to give a heavy plastic deformation. "Successfully" means that 5 successive time steps of 20 hours each gave closely the same plastic deformation.

4.4. Input

The input consists of specifications of geometry, materials properties and, for each point in time, fuel normal and friction force distributions, temperature distribution and axial stress. Further, a set of points in space must be defined in which to apply Nichols' model for the deformation rates.

4.5. Output

The output consists of the radial and axial displacements, the 4 non-vanishing strain components, the 4 non-vanishing stress components, both elastic and plastic, for a number of spatial points and for each point in time. The spatial points are coincident with those specified for application of Nichols' model.

5. Aspects of the Approach

With the options available (see paragraph 4.2) it is possible to treat both cladding segments and free fuel pellets.

With a few modifications it will be possible to treat interacting fuel pellets as well. This requires only the added capability of matching the normal and shear stresses on the outer surface with non-zero, specified distributions.

Thus, the approach provides a tool for handling nearly all axisymmetric cases of fuel and pellet mechanical and thermal loading and interaction, within the limitations inherent in the method.

The code consists of subroutines which may conveniently be integrated into future fuel performance models.

6. Comparison with Selected Data

Two types of calculations have been subjected to comparison against available data:

I. Uniform Heating and Pressurization

The cases of uniform heating and of pressurization can be solved rigorously. The mathematical solutions have been derived and the results compared to those generated by the model. The agreement was perfect.

II. Free Pellet Calculations

This type of calculation involves a parabolic radial temperature distribution. There are no direct measurements available of pellet deformations, only corresponding ridge heights. Veeder[4] has used basically the same calculational technique as the present model and compared his results successfully to ridge height data. It was therefore decided to compare the present model with Veeder's model for this type of calculation. Two cases were run, with length/radius = 1 and 2, respectively.

The results used from Veeder's model refer to a solid cylinder. The results used from the present model refer to a cylinder with a narrow central hole, since the model does not allow an inner radius of zero. The ratio of inner radius to outer radius, however, was made as small as 0.02.

For the case of length/radius = 2, Veeder's model shows a characteristic effect of the radial displacement at the center being greater than the minimum radial displacement. This is thought to be due to the capability of Veeder's model to accommodate a hydrostatic pressure at the pellet center. The present model does not produce this effect because of condition V. Veeder also reports cases of hollow cylinders, and in those cases the above effect is not present.

Considering these circumstances, the agreement is found to be very reasonable:

	Length/diameter = 1		Length/diameter = 2	
	Veeder's model	Present model	Veeder's model	Present model
Max. radial displacement (μ)	110	118	121	130
Center radial displacement (μ)	62	53	74	48
Min. radial displacement (μ)	62	53	67	48
Axial displacement at axis (μ)	114	193	201	409
Axial displacement at surface (μ)	40	4	124	23

7. List of Symbols

r,z	Cylindrical coordinates
s,t	Normalized cylindrical coordinates
r_1, r_2	Inner and outer radius of segment
L	Length of segment
u,v,w	Radial, circumferential and axial displacements
up, wp	Radial and axial plastic displacements
β_r, β_θ, β_a	Components of body force
σ_r, σ_θ, σ_a	Components of normal stress
$\sigma_{a\theta}$, $\sigma_{\theta r}$, σ_{ra}	Components of shear stress
i,j	Used to generalize indices of various types
ε_{ij}	Components of deformation
$^l_{ij}$	Components of elastic deformation
$^e_{ij}$	Components of plastic deformation
σ_{a0}	Applied axial stress
ρ	Density
E	Elastic modulus
ν	Poisson's ratio
G	Shear modulus = $E/2/(1+\nu)$
α	Temperature coefficient
T	Temperature change
W	Internal elastic energy
F,G,H,L,M,N	Anisotropy constants
P	Plastic modulus
σ_e	Effective stress
a_{ij}	Coefficients of u-polynomial
b_{ij}	Coefficients of w-polynomial
ap_{ij}	Coefficients of up-polynomial
bp_{ij}	Coefficients of wp-polynomial
P_1	Internal pressure
P_2	External pressure
K_n	Fuel normal force
K_s	Fuel friction force
M_1	Moment of axial stress at ridge top
M_2	Moment of axial stress at z = L
M_h	Moment of hoop stress
M_x	Moment of external load

8. References

1) R. Hill: A theory of the yielding and plastic flow of anisotropic metals, Roy. Soc. Proc., 193A, 281 (1948).

2) R. von Mises: Mechanik der plastischen Formänderungen von Kristallen, Zeitschrift für angewandte Matematik und Mechanik, June 1928.

3) F.A. Nichols: Theory of the creep of Zircaloy during Neutron Irradiation, J. Nuc. Mat., 30, 249 (1969).

4) J. Veeder: Thermo-Elastic Expansion of Finite Cylinders, AECL-2660, 1967.